

31. DATA REPORT: MOLECULAR AND STABLE ISOTOPE ANALYSES OF SORBED AND FREE HYDROCARBON GASES OF LEG 146, CASCADIA AND OREGON MARGINS¹

Michael J. Whiticar² and Martin Hovland³

INTRODUCTION

The collection and analysis of sediment gases, including light hydrocarbons, sulfur, and permanent gases, is a required routine during Ocean Drilling Program (ODP) drilling operations with the *JOIDES Resolution*. These measurements are a critical component of the shipboard safety and environmental protection conducted by the shipboard organic geochemists and ODP geochemistry technical staff. In addition, these gas analyses, in particular the hydrocarbons, are a valuable measurement asset for various scientific aspects of ODP investigations. This is because these gases are ubiquitous and diagnostic for many subsurface processes. For example, during Leg ODP 146 on the basis of determinations of the C₁–C₆ hydrocarbons (methane through hexane) it was possible to:

1. Differentiate between the occurrences of bacterial and thermogenic gases;
2. Identify autochthonous vs. allochthonous (i.e., migrated) gases;
3. Signal the approach and presence of free gases (e.g., associated with gas hydrate dissociation);
4. Pinpoint active fractures or fault zones or seepages with fluid and/or gas flow; and
5. Define the subsurface diagenetic and catagenetic regimes.

The shipboard characterization of the gases is based on concentration and molecular ratios, obtained by gas chromatography (GC). However, a more reliable classification of hydrocarbons found unexpectedly involves the shore-based determination of the stable carbon isotope ratios of the hydrocarbons, particularly methane. The combination of ²H/¹H and ¹³C/¹²C ratios of methane are especially powerful at discriminating between bacterial, thermogenic, geothermal, hydrothermal, and abiogenic methane (Fig. 1). In concert with the molecular and concentration data, the ¹³C/¹²C ratios of light hydrocarbons can also identify secondary alterations such as mixing or microbial oxidation (Fig. 2).

Additional gas characterization with molecular and stable carbon isotopes is provided by differentiating (1) dissolved or free gases in the interstices of the sediment from (2) the gases bound or sorbed on the organics and minerals in the sediments. Over the past 15 years, the Bundesanstalt für Geowissenschaften und Rohstoffe (BGR-method) Hannover, FRG has pioneered the development of measurement methodologies and interpretative schemes to take advantage of the gas genetic information contained in both the free and sorbed phases in sediments (e.g., Faber and Stahl, 1984). The use of sorbed and free gas analyses has been applied successfully on several ODP legs, in-

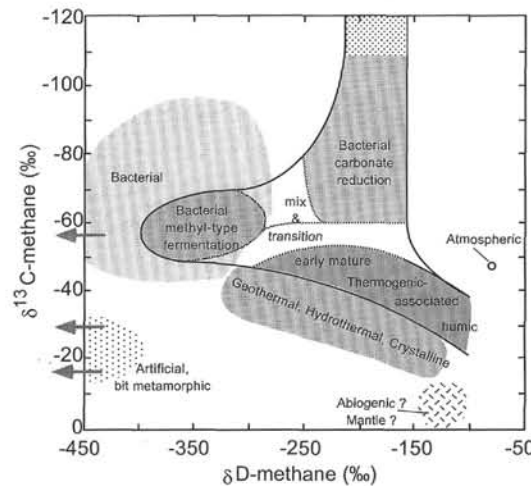


Figure 1. Gas classification diagram using the combination of stable carbon and hydrogen isotope ratios of methane (after Whiticar, 1990).

cluding Legs 104 (Whiticar and Faber, 1989), 112 (Whiticar and Suess, 1990), and 139 (Whiticar et al., 1994).

This is a data report of the light hydrocarbons encountered during drilling on the Cascadia and Oregon Margins. Some of this information is contained in the individual site chapters in the *Initial Reports* volume of Leg 146 (Westbrook, Carson, Musgrave, et al., 1994). Here, we document and make available our new shore-based data, which include:

1. Ratios of ¹³C/¹²C methane for selected Vacutainer® samples (free gas);
2. Development of a new sorbed/total gas extraction apparatus, in conjunction with this ODP Leg 146 investigation;
3. Concentrations of total methane in sediments by acid-vacuum gas desorption; and
4. Ratios of ¹³C/¹²C total methane from desorbed sediment samples.

Detailed interpretation and reporting of these and other geochemical results will be provided in the companion synthesis paper of Whiticar et al. (this volume).

METHODS

The techniques used to collect and analyze the sediment gas during shipboard operations are described in Shipboard Scientific Party (1994, p. 30). These will be presented briefly here, along with a description of the new mechanical acid-vacuum gas desorption device for sorbed/total gas analysis.

¹Carson, B., Westbrook, G.K., Musgrave, R.J., and Suess, E. (Eds.), 1995. *Proc. ODP, Sci. Results*, 146 (Pt. 1); College Station, TX (Ocean Drilling Program).

²School of Earth and Ocean Sciences, University of Victoria, P.O. Box 1700, Victoria, British Columbia V8W 2Y2, Canada.

³Statoil, P.O. Box 300, N-4001, Stavanger, Norway.

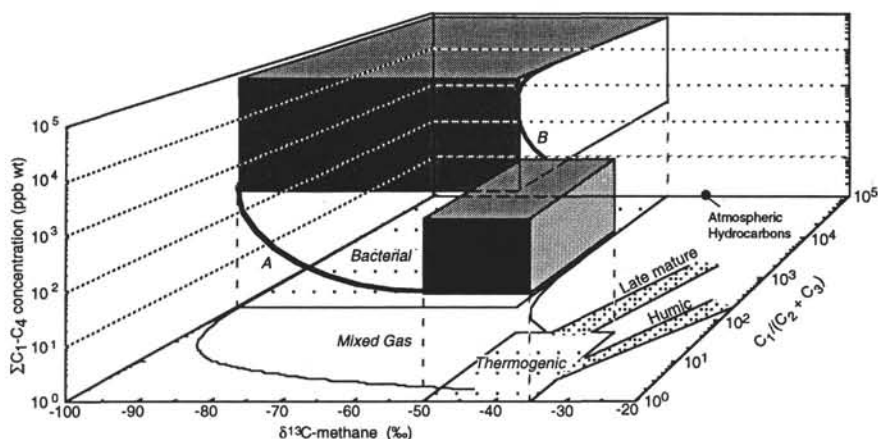


Figure 2. Three-dimensional natural gas classification diagram using the combination of stable carbon isotope ratios of methane, molecular $C_1/(C_2+C_3)$ ratios, and gas concentration (after Whiticar, 1990).

Sampling and Measurement for Headspace and Vacutainer Gases

During Leg 146, the compositions and concentrations of hydrocarbons and other gases were monitored in the sediments generally at intervals of one per core. Briefly, the two methods used are:

1. Headspace (HS) method:
 - a. 5-mL sediment core taken with a cork borer and sealed into a serum vial;
 - b. vial warmed to 60°C;
 - c. aliquots of gas released by the sediments analyzed by GC.
2. Vacutainer (V) or expansion void gas (EVG) method:
 - a. samples taken on catwalk into pre-evacuated glass Vacutainers when gas pockets or expansion voids occurred in cores as they arrived on deck;
 - b. aliquots of gas analyzed by GC.

Gas Chromatographic Systems

The two systems used were the (1) Hach-Carle AGC Series 100 (Model 211), a standard packed column isothermal flame ionization detector (FID) GC, attached to Hewlett-Packard Model 3393A Integrator; and (2) the Hewlett-Packard 5890A Natural Gas Analyzer, modified by John Booker & Company, Austin, Texas, modified multivalve and multicolumn, temperature-programmed GC equipped

with both thermal conductivity (TCD) and FID, and two Hewlett-Packard Model 3393A Integrators dedicated to the TCD and FID.

Sampling and Measurement for Total and Sorbed Gases

Sediment samples for the sorbed and total hydrocarbons were obtained from the sediments collected for interstitial fluids (see Shipboard Scientific Party, 1994, p. 32). The sediment was frozen immediately after subsectioning and stored frozen until analysis.

The previous BGR-method used to desorb gases from sediments required 100–200 of sediment and a bulky glass vacuum extraction line (Faber and Stahl, 1984). This was necessary in order to obtain at least 50 nmol of CH_4 for the $^{13}C/^{12}C$ determination by conventional isotope ratio mass spectroscopy (IRMS). With the development of the on-line, gas chromatograph/combustion/isotope ratio mass spectrometer (GC/C/IRMS) (Fig. 3), we are now able to measure $^{13}C/^{12}C$ on extremely small quantities of methane (~100 picomole, Whiticar and Cederberg, in press). This reduction in the amount of gas required also reduced the amount of sediment need to be degassed, and hence the degassing apparatus. Details of the new method are reported by Whiticar (in press).

Figure 4 shows the new sorbed gas desorption device. It consists of a thick-walled glass reaction vessel, with a three-port lid sealed by an O-ring/clamp. The lid provides for a transducer measurement of pressure/vacuum, and a valve-septum arrangement for addition of solutions and removal of gas samples. The procedure is briefly described below.

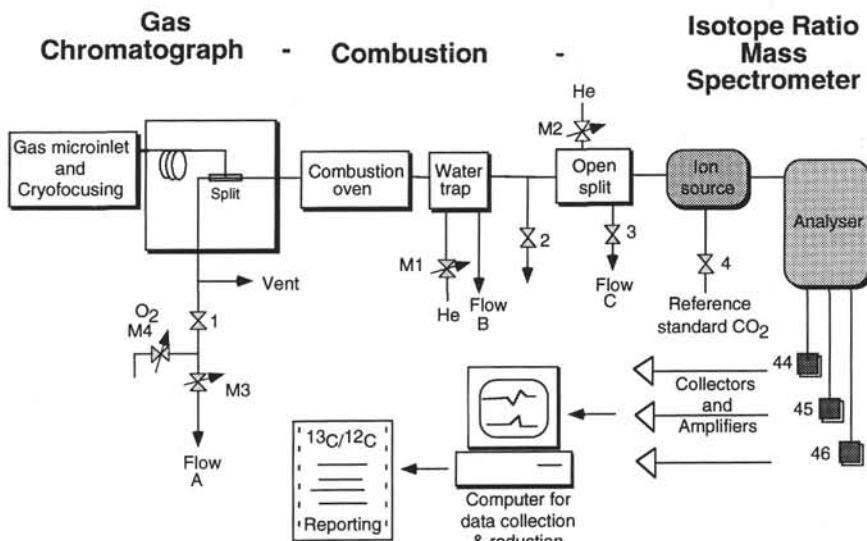


Figure 3. Basic schematic of GC/C/IRMS instrumental configuration for stable carbon isotope ratios of Vacutainer and total methane (after Whiticar and Cederberg, in press).

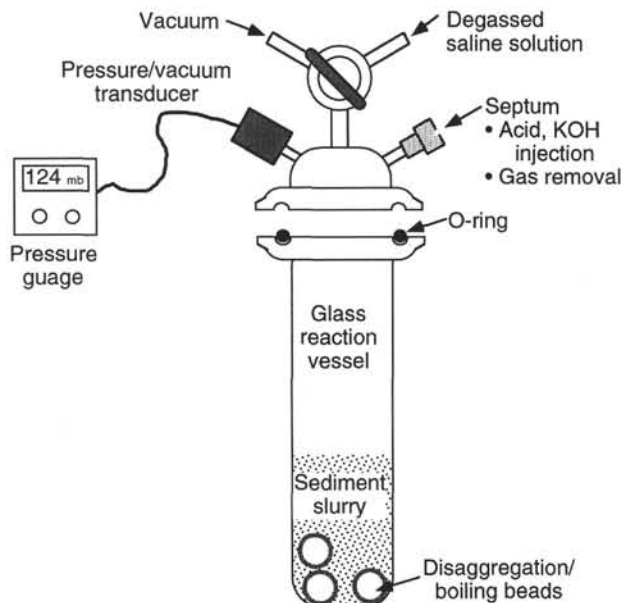


Figure 4. Light hydrocarbon acid/vacuum sediment gas desorption device (after Whiticar, in press).

A known weight of frozen sediment, typically 1–5 g wet sediment, is thawed under vacuum in the apparatus. Enough saline solution (degassed water saturated with NaCl) is added to make a slurry using a vortex mixer. Phosphoric acid is added slowly to release the sorbed gas fraction into the headspace. At the same time some carbonates will dissolve and generate free CO₂. It is the carbonate content of the sediment, and hence amount of CO₂ released that limits the practical sample size. The vessel is immersed in a water bath and the slurry is brought to a boil under reduced pressure (~75°C, 200 mbar). KOH is added to precipitate the CO₂, leaving the desorbed hydrocarbons and some N₂, O₂, CO₂, H₂O, and possibly H₂S in the headspace of the reaction vessel. The vessel is brought to atmospheric pressure with degassed saline solution. Aliquots of gas are taken for analysis. Gases are then analyzed by conventional GC or by GC/C/IRMS. At our current stage of the method development, it is still possible that a portion of the free gas could be contained in the sorbed gas fraction. Because of this, we refer to this analysis at this stage as a total gas analyses. Continued evolution of this method will effectively eliminate the free gas fraction.

Concentration Units and Notation

The gases measured by the headspace and Vacutainer/EVG methods are reported on a gas volumetric basis, in parts per million by volume (ppmv), e.g., μl CH₄/L sample. In the case of the Vacutainer/EVG the partial pressures of the gases measured are similar to those in the gas pocket of the sediment core liner. Inherent in the sampling for the headspace measurement, there is considerable contamination of air in the vial prior to sealing. Hence, the abundances are only proportional or relative. The concentration of methane in the sorbed gases is reported on a wet-sediment weight basis, i.e., μg CH₄/kg wet sediment (ppb wt).

Stable Isotope Notation

For practical reasons, stable isotope data are determined as a ratio, for example, ¹³C/¹²C, rather than as an absolute molecular abundance, and are reported as the magnitude of excursion in per mil of the sam-

ple isotope ratio relative to a known standard isotope ratio. The usual δ-notation generally used in the earth sciences is:

$$\delta^{13}\text{C}(\text{\textperthousand}) = \frac{{}^{13}\text{C}/{}^{12}\text{C}_{\text{sample}} - {}^{13}\text{C}/{}^{12}\text{C}_{\text{standard}}}{{}^{13}\text{C}/{}^{12}\text{C}_{\text{standard}}} \times 10^3 \quad (1)$$

where the ¹³C/¹²C isotope ratio is referenced relative to the PDB standard.

RESULTS

Only the basic analytical results are presented in the following tables and figures. Readers interested in interpretative aspects and discussion regarding the data should refer to Whiticar et al. (in press and this volume), and Hovland et al. (this volume).

Hole 888B, Cascadia Margin

The results of the headspace, Vacutainer, and total gas analyses for Hole 888B are presented in Tables 1–3, respectively. Representative depth plots for the methane concentrations and δ¹³C_{methane} are shown in Figures 5 and 6.

Hole 889A, Cascadia Margin

The results of the headspace, Vacutainer, and total gas analyses for Hole 889A are presented in Tables 4–6, respectively. Representative depth plots for the methane concentrations and δ¹³C_{methane} are shown in Figures 7 and 8.

Hole 891B, Oregon Margin

The results of the headspace, Vacutainer, and total gas analyses for Hole 891B are presented in Tables 7 and 8. Representative depth plots for the methane concentrations and δ¹³C_{methane} are shown in Figures 9 and 10.

Site 892, Oregon Margin

The results of the headspace, Vacutainer, and total gas analyses for Site 892 are presented in Tables 9–11, respectively. Representative depth plots for the methane concentrations and δ¹³C_{methane} are shown in Figures 11 and 12.

ACKNOWLEDGMENTS

We would like to thank F. Harvey-Kelly for the desorption laboratory work and T. Cederberg for operation of the GC/C/IRMS. The sorbed gas analyses were supported by a Nordic Research grant to M.H. The GC/C/IRMS facility was funded largely by a grant to M.J.W. by NSERC Strategic (STR0118459) and Operating (OPG0105389) Grants.

REFERENCES

- Faber, E., and Stahl, W., 1984. Geochemical surface exploration for hydrocarbons in North Sea. *AAPG Bull.*, 68:363–386.
- Shipboard Scientific Party, 1994. Explanatory notes. In Westbrook, G.K., Carson, B., Musgrave, R.J., et al., *Proc. ODP, Init. Repts.*, 146 (Pt. 1): College Station, TX (Ocean Drilling Program), 15–48.
- Westbrook, G.K., Carson, B., Musgrave, R.J., et al., 1994. *Proc. ODP, Init. Repts.*, 146 (Pt. 1): College Station, TX (Ocean Drilling Program).
- Whiticar, M.J., 1990. A geochemical perspective of natural gas and atmospheric methane. In Durand, B., and Behar, F. (Eds.), *Advances in*

Organic Geochemistry 1989, Part I. Organic Geochemistry in Petroleum Exploration. Org. Geochem., 16:531–547.

, in press. An acid/vacuum micro-extraction device for molecular and stable isotopic analysis of free and sorbed sediment gases. *Anal. Chem.*

Whiticar, M.J., and Cederberg, T., in press. Stable carbon isotope determinations of hydrocarbon gases at the picomole level by GC-C-IRMS. *Anal. Chem.*

Whiticar, M.J., and Faber, E., 1989. Molecular and stable isotope composition of headspace and total hydrocarbon gases at ODP Leg 104, Sites 642, 643, and 644, Vøring Plateau, Norwegian Sea. In Eldholm, O., Thiede, J., Taylor, E., et al., *Proc. ODP, Sci. Results*, 104: College Station, TX (Ocean Drilling Program), 327–334.

Whiticar, M.J., Faber, E., Whelan, J.K., and Simoneit, B.R.T., 1994. Thermogenic and bacterial hydrocarbon gases (free and sorbed) in Middle Valley, Juan de Fuca Ridge, Leg 139. In Mottl, M.J., Davis, E.E., Fisher, A.T., and Slack, J.F. (Eds.), *Proc. ODP, Sci. Results*, 139: College Station, TX (Ocean Drilling Program), 467–477.

Whiticar, M.J., and Suess, E., 1990. Characterization of sorbed volatile hydrocarbons from the Peru margin, Leg 112, Sites 679, 680/681, 682, 684, and 686/687. In Suess, E., von Huene, R., et al., *Proc. ODP, Sci. Results*, 112: College Station, TX (Ocean Drilling Program), 527–538.

Date of initial receipt: 12 September 1994

Date of acceptance: 12 April 1995

Ms 146SR-212

Table 1. Headspace analyses for Hole 888B.

Core, section, interval (cm)	Depth (mbsf)	O ₂	N ₂	CH ₄	CO ₂	C ₂ H ₆	C ₃ H ₈	C ₁ /C ₂	C ₁ /C ₂₊
1H-1, 5–55	0.3	62	380	1.2	373			1E+6	1E+6
1H-1, 58–108	0.8	65	402	0.9	158			1E+6	1E+6
1H-1, 111–161	1.4	1,490	1,388	2.0	433			1E+6	1E+6
1H-2, 164–214	3.4	70	428	1.4	2			1E+6	1E+6
1H-3, 0–5	3	27,736	116,760	3.2	4,954			1E+6	1E+6
1H-3, 50–53	3.5	18,479	80,024	3.8				1E+6	1E+6
2H-4, 50–53	11	2,534	4,991	6.2	3,733			1E+6	1E+6
2H-6, 0–5	13	6,862	31,144	4.1	95			1E+6	1E+6
3H-5, 0–5	21	4,330	16,148	3.3	1,385			1E+6	1E+6
4H-5, 0–5	31	2,536	4,803	4.0	96			1E+6	1E+6
5H-5, 0–5	40	93	568	2.7	3			1E+6	1E+6
6H-6, 0–5	51	3,622	8,709	1.5	9			1E+6	1E+6
7H-5, 0–5	59	2,459	4,224	4.4	52			1E+6	1E+6
8H-5, 0–5	69	2,572	4,609	4.1				1E+6	1E+6
9H-4, 0–5	77	21,125	89,807	1.0	24,73			1E+6	1E+6
9H-4, 147–150	78	93	570	0.4	5			1E+6	1E+6
10H-5, 0–5	88	1,701	1,539	110.5	4,795			1E+6	1E+6
11H-2, 0–5	93	6,666	28,959	150.9	1,384			1E+6	1E+6
11H-3, 0–5	94	1,557	1,402	91.2	5,156			1E+6	1E+6
12H-3, 0–5	104	240,916		4.4	9,014			1E+6	1E+6
13H-4, 0–5	113	13,635	59,395	0.8	82			1E+6	1E+6
14H-5, 0–5	124	302,313		0.7	4,744			1E+6	1E+6
15H-3, 0–5	131	39,868	165,777	0.4	77			1E+6	1E+6
16H-6, 0–5	145	1,313	1,224	0.7	1,279			1E+6	1E+6
17H-5, 0–5	153	4,224	14,061	1.5	63			1E+6	1E+6
18X-5, 0–5	162	22,574	95,665	0.2				1E+6	1E+6
19X-5, 0–5	172	1,633	2,566	0.3	493			1E+6	1E+6
20X-1, 0–5	175	3,873	11,831	3.6	190			1E+6	1E+6
21X-1, 0–2	185	245,792		0.3	29			1E+6	1E+6
24H-2, 0–5	214	1,877	2,256	438.4	419			1E+6	1E+6
25H-4, 0–5	222	6,333	28,803	622.5	3,640			1E+6	1E+6
26H-2, 0–5	228	8,519	38,199	5,997.2	49			1E+6	1E+6
26H-4, 0–5	236	864	921	5,930.9	1,025			1E+6	1E+6
27H-5, 0–5	240	22,357	95,014	6,710.4	77			1E+6	1E+6
28H-2, 0–5	245	18,518	4,570	6,862.5	3,327			1E+6	1E+6
29H-4, 0–5	256	3,231	7,809	4,120.9	941			1E+6	1E+6
30H-1, 145–150	262	238,036		2,447.8	4,093			1E+6	1E+6
30H-5, 0–5	267	2,434	4,466	6,238.6	4,062			1E+6	1E+6
31H-6, 0–5	275	347,059		3,969.2	3,667			1E+6	1E+6
34H-1, 127–130	294	171,925		8,586.7	1,107			1E+6	1E+6
34H-5, 0–5	298	1,174	1,136	8,967.1	1,236			1E+6	1E+6
35H-4, 0–5	305	6,790	31,270	8,059.9	2,129			1E+6	1E+6
35H-5, 0–5	307	4,570	18,653	23,241.0	2,955			1E+6	1E+6
36H-2, 65–70	312		1	4,123.0	51			1E+6	1E+6
37H-7, 36–40	329	409,891		6,525.2	3,070			1E+6	1E+6
40H-3, 0–5	351	290,869		68,043.0	2,331			1E+6	1E+6
41X-1, 0–5	357	3,903	12,114	14,107.0	56			1E+6	1E+6
42X-1, 2–3	367	126,046	29,812	950.1	1,581			1E+6	1E+6
43X-1, 0–5	376	20,811	89,179	33,329.0	1,058			1E+6	1E+6
44X-3, 145–150	390	356,547		20,264.0	5,381			1E+6	1E+6
45X-2, 0–5	397	582,869		8,309.5	1,129			1E+6	1E+6
47X-1, 0–2	414	572,548		10,031.0	4,012			1E+6	1E+6
48X-1, 0–5	424	503,233		28,517.0	6,002			1E+6	1E+6
50X-1, 20–24	443	404,321		5,017.1	80			1E+6	1E+6
52X-1, 20–25	452	1,838	2,080	5,199.9	68			1E+6	1E+6
53X-1, 48–53	461	41	250	13,918.0	6			1E+6	1E+6
54X-2, 0–5	471	1,136	1,136	1,342.4				1E+6	1E+6
55X-1, 0–5	478	15,321	66,570	8,978.4	1,888			1E+6	1E+6
56X-1, 40–45	488	3,391	7,761	5,718.5				1E+6	1E+6
57X-1, 137–140	498	24,508	103,165	18,712.0	62			1E+6	1E+6
58X-2, 145–150	508	510,48	208,69	24,246.6	2			1E+6	1E+6
59P-1, 0–5	514	1,120	1,061	2,952.1				1E+6	1E+6
59P-1, 47–48	514	18,263	77,182	582.7	155			1E+6	1E+6
60X-1, 0–5	515	4,150	13,898	19,026.0		1.0		20,006	20,006
61X-1, 145–150	524	17,656	74,510	18,223.0		1.2		15,123	15,123
62X-2, 0–5	533	2,109	3,204	2,189.8	37			1E+6	1E+6
63X-2, 0–5	542	6,437	27,285	11,704.0	2,616	1.4		8,587	8,587
64X-2, 0–5	551	9,390	40,152	2,848.0		1.3		2,243	2,243
65X-4, 145–150	564	20,984	88,681	2,850.0		2.2	0.7	1,272	986

Table 2. Vacutainer analyses for Hole 888B.

Core, section, interval (cm)	Depth (mbsf)	O ₂	N ₂	C ₁	CO ₂	C ₂	C ₃	nC ₄	nC ₅	nC ₆	C ₁ /C ₂	C ₁ /C ₂₊
31H-3, 100–103	271.82	2,851.6	5,865	65.55	55.1	1.65	1.4	9.6	2.2	1.1	3.97E + 1	4
36H-7, 0–1	319.01			50	373.2						1.00E + 6	1E + 06
44H-3, 38–39	398.89	19,669	84,902	586,879	95	14.67	2.6				4.00E + 4	33,983
44H-4, 143–144	401.44	453,492	380	173,705	1600	3.4					5.11E + 4	51,090
62H-3, 108–109	535.79	27.4	163.3	450,158	9.1	23.57	1				1.91E + 4	18,321

Table 3. Total gas analyses for Hole 888B.

Core, section, interval (cm)	Depth (mbsf)	CH ₄ (ppb)	ng CH ₄ /g sediment	$\delta^{13}\text{CH}_4$ (‰)
3H-2, 145–150	18	228	-39.8	
8H-4, 140–150	68.4	197	-41.8	
9H-3, 140–150	76.4	309	-43.2	
9H-3, 140–150	76.4	284	-42.1	
10H-4, 140–150	87.4	156	-43.2	
11H-3, 142–152	95.3	231	-37.5	
14H-4, 138–150	124	203	-33.9	
18H-4, 135–150	159	151	-34.5	
24H-1, 135–150	214.3	193	-38.7	
24H-1, 135–150	214.3	171	-33.4	
34H-2, 130–150	293.7	99	-52.4	
34H-2, 130–150	293.7	31	-50.7	
34H-2, 130–150	293.7	29	-48.8	
36H-2, 70–80	312.2	631	-59.9	
48X-CC, 0–5	423.5	350	-57.4	
61X-1, 1–10	522.8	409	-50.3	
63X-2, 130–150	543.2	253	-50.6	
63X-2, 130–150	543.2	414	-51.7	
65X-5, 0–25	564.1	204	-50.4	

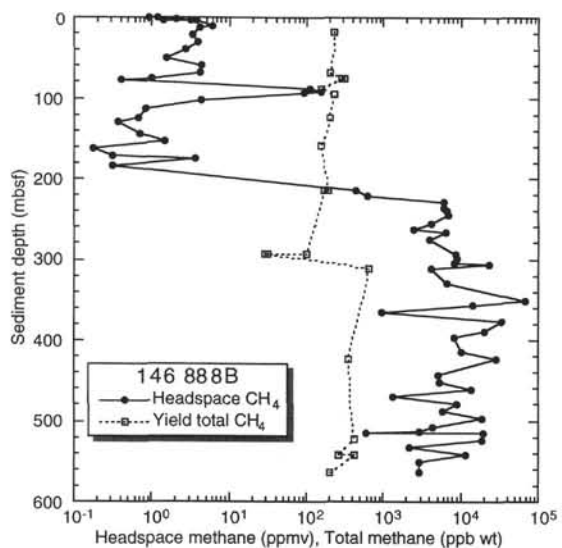


Figure 5. Depth distribution of headspace methane and total methane concentrations at Hole 888B.

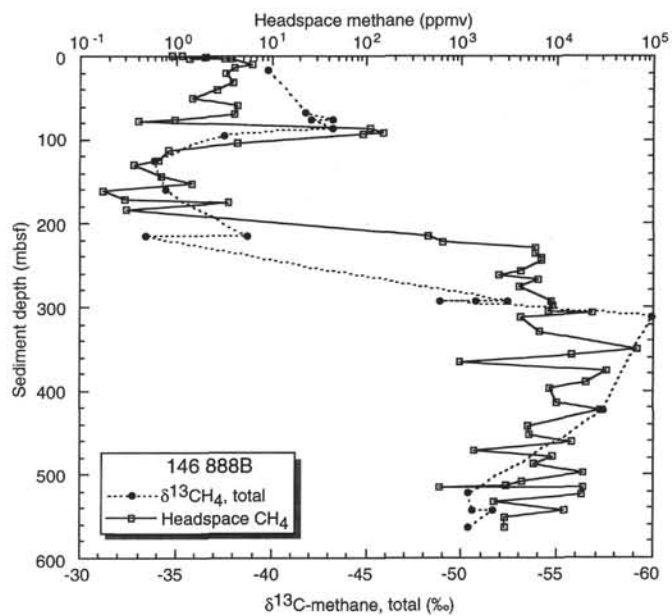


Figure 6. Depth distribution of total methane carbon isotope ratio and headspace methane concentrations at Hole 888B.

Table 4. Headspace analyses for Hole 889A.

Core, section, interval (cm)	Depth (mbsf)	O ₂	N ₂	C ₁	CO ₂	C ₂	C ₃	iC ₄	nC ₄	C ₁ /C ₂₊
1H-2, 0–6	21.5	19	114	58,980	1.2	1.4				42,129
1H-5, 0–5	26.0	96	585	60,149	3.6	1.5				40,099
2H-1, 145–150	31.0	1,295	1,231	50,134	2.2	2.4				20,889
2H-5, 140–145	36.9	94	577	31,452	4,386	1.3				24,194
3H-1, 145–150	40.5	353	713	30,622	3.27	1.6			1.9	8,749
3H-6, 6–10	46.6	79	491	49,953	823.1	1.9		3.6	0.9	7,805
4H-3, 0–5	51.5	34.7	208	11,914	65.5	1.1				10,831
4H-6, 0–5	56.0	416	724	22,312	47.9	1.6				13,945
5H-4, 0–5	62.5	60	369	33,126	16	2.4				13,803
6H-6, 0–5	75.0	77.9	481	48,830	65.5	2.9				16,838
7H-2, 0–5	78.5	41.7	268	23,922	7.3	2.4				9,968
8H-4, 0–5	91.0	25	150	12,225	1.3	1.1				11,114
9H-4, 0–5	99.0	2,217	3,501	21,412	23.5	2.3				9310
10H-4, 150–152	110.0	3,661	9,217	9,652	39.3	2.2				4,387
11H-2, 0–5	115.0	6,093	26,875	27,858	1,662	4.6				6,056
12H-2, 0–5	120.5	4,143	13,472	9,652	1,921	2.2				4,387
13H-1, 0–5	127.0	9,055	40,702	76,498	1,634	14.1				5,425
14H-1, 148–153	129.5	8,356	36,951	10,053	1,770	11.2				898
15P-1, 45–50	129.5	2,103	3,089	51,184	1,898	33.4				1,532
17X-2, 75–80	132.4	50,123	208,641	60,798	3,644	20.2	0.35			2,959
18X-4, 31–36	144.4	58,023	237,429	46,432	6,325	12.5	1.66			3,279
19X-3, 145–150	153.6	25,010	109,405	48,534	1,923	19.25	0.55			2,451
20X-3, 133–138	163.0	33,101	140,520	54,756	1,758	12.6	0.6			4,148
22X-2, 0–5	179.0	4,255	15,273	30,784	1,383	9.5	0.7			3,018
24X-6, 0–5	195.3	4,061	12,777	47,330	3,792	22.3	3.4			1,842
25X-2, 145–150	200.3	3,965	11,814	48,662	3,185	16	1.7			2,749
26X-3, 0–5	209.8	2,926	6,447	47,192	3,300	20.5	2.2			2,079
28X-3, 0–5	220.3	3,748	10,249	71,222	2,035	33.3	2.7			1,978
30X-3, 0–5	230.8	3,141	7,260	45,859	33,229	38.8	1.9			1,127
31X-3, 0–5	240.2	1,986	2,669	74,882	3,294	35.9	1.3			2,013
32X-1, 125–130	248.0	2,161	3,223	10,042		12.78				786
32X-3, 0–5	249.7	60,347	249,019	10,055	982	12.15				828
34X-2, 145–150	260.2	25,160	108,685	16,271	1,824	24.75	1.06			630
36X-1, 94–99	267.7	184,462	860,777	23,299	10,299	35.66	1.7			624
37X-1, 0–1	275.2	2,522	4,859	34,004	2,449	35.3	0.59			947
38X-1, 0–1	284.1	73,520	300,328	42,402	1,054	48.9	1.4			843
39X-1, 45–50	293.3	15,283	66,932	10,077	1,898	35.8	0.81			275
40X-3, 0–5	301.5	4,173	14,104	25,619	1,811	58.3	0.72			434
40X-4, 39–44	301.5	3,298	7,850	26,463	2,487	134	1.6			195
41X-5, 0–5	310.5	7,872	34,327	38,529	1,124	83	1.1			458
42X-1, 42–44	319.5	51,386	212,776	8,929	963	108.9	1.6			81
43X-2, 0–5	328.4	43,413	180,977	44,390	2,109	110.1	0.99			400
44X-1, 101–106	337.2	16,318	71,628	29,687	2,233	225.2	1.4			131

Table 5. Vacutainer analyses for Hole 889A.

Core, section, interval (cm)	Depth (mbsf)	Type	C ₁	C ₂	C ₃	Area (Vs)	δ ¹³ CH ₄ (‰)	Area (Vs) repl.	δ ¹³ CH ₄ (‰)
1H-1, 41–42	20.4	V	812,418.7	31.8	0.3	8.6	-84.4	12.0	-83.6
4H-2, 132–133	51.3	V	962,874.0	65.8	0.6	16.3	-66.2		
5H-7, 37–38	82.2	V	995,485.3	83.5	0.6	19.9	-61.5	12.9	-61.5
9H-8, 91–92	113.1	V	562,284.0	62.7	1.5	8.8	-57.1		
12H-5, 5–6	125.1	V	464,676.0	211.7	1.0	9.0	-56.7		
19X-3, 140–141	144.5	V	782,283.9	607.2	2.6	9.4	-53.6		
20X-3, 90–91	162.5	V	969,920.4	522.7	6.7	5.0	-50.8		
22X-6, 28–29	185.3	V	892,816.0	866.9	9.2	5.3	-49.9	7.6	-50.4
25X-2, 100–101	199.8	V	798,851.4	687.4	7.7	7.3	-50.7		
26X-4, 56–57	211.9	V	867,673.0	625.4	6.5	7.0	-50.3		
28X-4, 101–102	222.8	V	813,107.7	867.3	5.1	13.0	-51.0		
30X-2, 81–82	230.1	V	894,792.1	775.7	4.1	11.5	-53.7	10.6	-53.8
31X-5, 51–52	243.7	V	733,235.5	412.2	3.7	10.0	-54.9		
40X-1, 102–103	302.5	V	218,779.0	206.1	1.0	8.0	-49.5		
41X-4, 35–36	315.4	V	860,362.1	2,813.5	5.0	14.5	-47.4	9.5	-47.3
103/VAC7000004/1		Lab standard	700,000.0	87,500.0	52,500.0	8.7	-36.4		
103/VAC7000004/2		Lab standard	700,000.0	87,500.0	52,500.0	13.8	-36.6		
103/VAC7000004/3		Lab standard	700,000.0	87,500.0	52,500.0	7.2	-37.1		
103/VAC7000004/4		Lab standard	700,000.0	87,500.0	52,500.0	11.3	-36.5		
103/VAC7000004/1		Lab standard	700,000.0	87,500.0	52,500.0	8.7	-36.4		
103/VAC7000004/2		Lab standard	700,000.0	87,500.0	52,500.0	13.8	-36.6		

Note: repl. = replicate analysis.

Table 6. Total gas analyses for Hole 889A.

Core, section, interval (cm)	Depth (mbsf)	Type	Weight (g) frozen sediment	Area (Vs)	$\delta^{13}\text{CH}_4$ (‰)	CH_4 (ppb wt) ng CH_4 /g frozen sediment
5H-1	102	VFG	9.25	3.2	-55.2	488
5H-1	102	VFG	9.15	3.96	-55.1	659
13H-2	129	VFG	8.18	15.45	-56.8	2,241
13H-2	129	VFG	8.18	14.14	-56.8	2,051
24X-5	198.8	VFG	4.8	9.02	-50.8	2,121
24X-5	198.8	VFG	4.8	8.37	-50.7	1,968
32X-3	248	VFG	7.89	2.03	-54.2	271
32X-3	248	VFG	7.89	1.87	-53.5	250
32X-3	248	VFG	6.85	1.8	-52.9	290
32X-3	248	VFG	6.85	1.64	-52.8	265
40X-4	306.47	VFG	2.34	0.78	-45.2	409
43X-2	329.8	VFG	12.57	1.08	-48.0	95
43X-2	329.8	VFG	12.57	2.65	-47.3	232

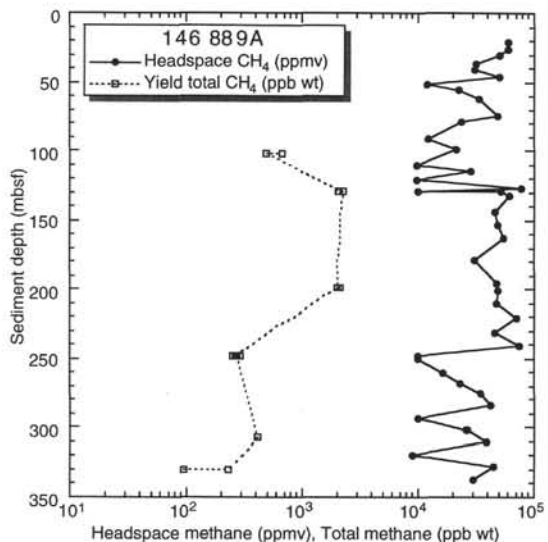


Figure 7. Depth distribution of headspace methane and total methane concentrations at Hole 889A.

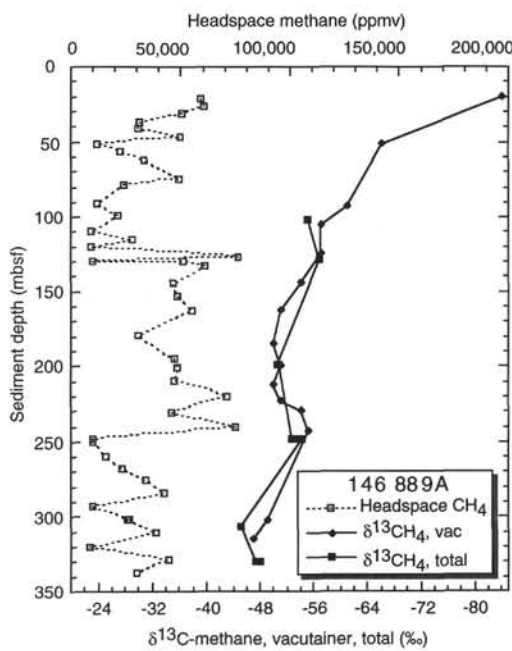


Figure 8. Depth distribution of Vacutainer and total methane carbon isotope ratio and headspace methane concentrations at Hole 889A.

Table 7. Headspace and Vacutainer analyses for Holes 891A and B.

Core, section, interval (cm)	Depth (mbsf)	O ₂	N ₂	CH ₄	CO ₂	C ₂ H ₄	C ₂ H ₆	C ₃ H ₆	iC ₄	nC ₄	C ₁ /C ₂
Headspace											
146-891A											
1H-3, 0-5	3.03	155,935	937,857	3	464						1E + 6
2H-2, 0-5	6.23	171,141	928,039	3	3,492						1E + 6
3H-2, 0-5	8.83	208,204	787,818	3	3,263						1E + 6
146-891B											
3X-CC, 0-2	20.81	142,183	963,534	4	1,501						1E + 6
4X-CC, 0-2	29.61	164,223	910,127	2	963						1E + 6
10X-1, 0-5	85.13	184,210	736,677	5	2,932						1E + 6
11X-2, 0-5	102.43	205,006	807,826	8	2,067						1E + 6
14X-1, 59-64	110.12	196,472	838,754	7	1,157						1E + 6
15X-1, 1-6	118.44	105,703	1,067,457	3	275						1E + 6
16X-1, 49-54	127.82	193,098	752,829	5	574						1E + 6
18X-CC, 7-9	145.18	170,089	910,598	2	2,320						1E + 6
19X-1, 8-10	153.99	184,488	75,319	2	1,158						1E + 6
20X-1, 142-147	164.15	193,889	750,667	16	3,767						1E + 6
21N-1, 47-52	172.10	178,763	727,660	2	1,877						1E + 6
22X-1, 62-67	176.75	188,927	742,200	2	1,318						1E + 6
23X-1, 145-150	181.98	182,443	787,209	3	1,328						1E + 6
25X-1, 56-61	198.79	171,084	731,476	2	2,550						1E + 6
26X-1, 10-15	207.23	146,819	1,059,769	4,658	4,133						1E + 6
27X-1, 10-15	216.03	205,096	806,067	944	5,463						1E + 6
28X-1, 45-50	225.18	198,732	843,058	9,135	3,570						1E + 6
30X-2, 85-89	239.97	191,709	827,795	10,065	629						1E + 6
31X-2, 0-5	243.93	102,125	469,106	9,924	23,399						1E + 6
32X-1, 20-25	251.63	164,332	772,866	40,864	13,805						44,082
33X-1, 20-25	260.43	171,706	713,942	31,428	6,102						1E + 6
34X-2, 50-53	265.12	147,363	775,640	49,033	16,379						39,258
35X-1, 145-150	270.48	171,123	717,895	20,321	7,018						1E + 6
37X-1, 0-4	278.82	190,979	906,506	34,758	8,407						1E + 6
38X-2, 0-5	287.93	155,194	979,326	50,886	13,315						57,175
39X-2, 0-5	296.63	208,975	908,710	56,915	23,235						45,899
40X-1, 0-5	304.03	201,758	795,865	9,383	9,230						1E + 6
41X-2, 0-5	314.33	116,760	507,611	25,447	94,796						5,718
42X-1, 147-150	323.09	163,534	717,869	37,572	8,466						1E + 6
43X-3, 0-5	333.43	150,716	749,949	16,873	3,878						1E + 6
44X-1, 9-14	339.42	175,525	918,771	18,593	5,739						1E + 6
45X-1, 0-5	348.23	204,890	853,129	41,835	5,529						1E + 6
47X-1, 65-75	366.80	123,153	615,195	10,034	27,688	0.3	1.0	tr.	tr.	tr.	1E + 4
48X-1, 47-49	375.48	173,957	699,399	25,524	4,346	tr.	tr.	tr.	tr.	tr.	1E + 6
49X-1, 0-5	383.93	176,610	749,105	17,756	3,875	tr.	tr.	tr.	tr.	tr.	1E + 6
50X-1, 0-5	392.83	140,605	649,341	17,240	1,070	tr.	tr.	tr.	tr.	tr.	1E + 6
52X-1, 21-26	410.74	161,044	958,588	6,357	39,090	tr.	1.8	2.0	1.2	3.7	3,512
55X-1, 35-40	437.38	173,406	805,778	40,129	15,686	tr.	1.0	tr.	1.3	2.1	38,960
56X-2, 0-5	447.33	171,160	921,846	36,946	7,946						1E + 6
57X-1, 48-53	455.21	203,585	860,335	33,387	13,596						1E + 6
58X-2, 27-32	465.30			32,258	3,403			tr.			1E + 6
Vacutainer											
146-891B											
41X-2, 98-99	315.29	109,703	442,017	58,430	468,343						390
42X-2, 50-50	323.60	198,221	812,857	6,597	1,312						6,597
47X-2, 49-49	368.09	181,257	691,711	34,502	87,728	3.5	4.7	2.6			7,325
55X-2, 107-108	368.68	209,046	792,808	197,281	2,579	3.5	2.4	2.6			82,200

Table 8. Total gas analyses for Hole 891B.

Core, section, interval (cm)	Depth (mbsf)	Type	Weight (g) frozen sediment	Area (Vs)	$\delta^{13}\text{CH}_4$ (‰)	CH ₄ (ppb wt) ng CH ₄ /g frozen sediment
56X-1, 72-89	446.52	VFG	1.05	0.5377	-50.7	563.1
55X-2, 130-150	438.97	VFG	1.41	0.8087	-63.4	659.5
55X-2, 130-150	438.97	VFG	1.41	0.7478	-64.0	609.8
52X-1, 7-21	410.57	VFG	1.09	0.3444	-38.7	427.7
52X-1, 7-21	410.57	VFG	1.09	0.3207	-39.4	398.3
43X-1, 10-27	330.50	VFG	1.36	0.5119	-44.2	446.9
43X-1, 10-27	330.50	VFG	1.36	0.4754	-42.9	415.0
41X-1, 135-150	314.15	VFG	0.81	0.3543	-42.6	530.9
21N-CC, 0-5	172.12	VFG	1.64	0.2148	-42.7	197.1
15X-1, 82-90	119.22	VFG	1.37	0.474	-37.7	461.5
Standard		V		14.5567	-36.6	
Standard		V		0.971	-36.6	

Note: VFG = Vacutaine Free Gas, V = Vacutainer, and Vs = GC/C/IRMS peak area mass 44 (Volt sec).

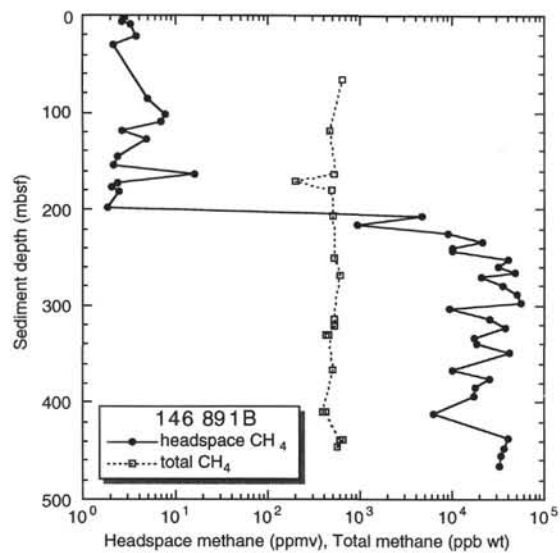


Figure 9. Depth distribution of headspace methane and total methane concentrations at Hole 891B.

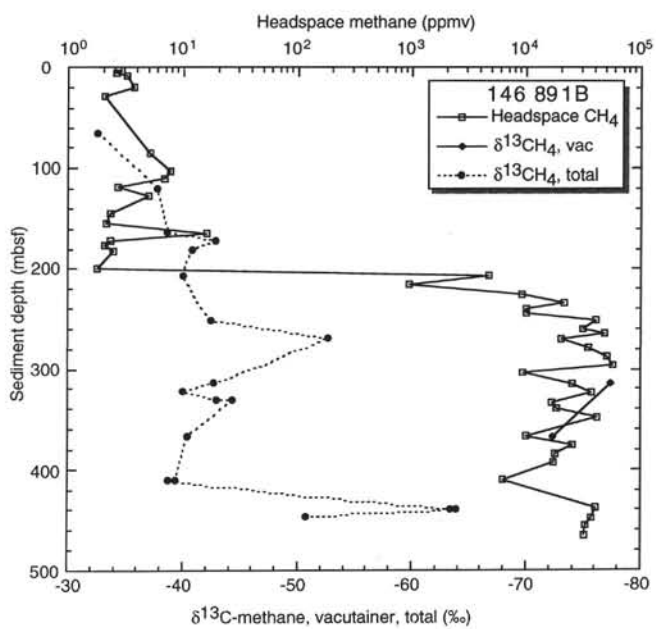


Figure 10. Depth distribution of total and Vacutainer methane carbon isotope ratios and headspace methane concentrations at Hole 891B.

Table 9. Headspace analyses for Holes 892A, 892D, and 892E.

Core, section, interval (cm)	Depth (mbsf)	O ₂	N ₂	CH ₄	CO ₂	C ₂ H ₄	C ₂ H ₆	H ₂ S	C ₃ H ₆	iC ₄	nC ₄	C ₁ /C ₂₊
146-892A												
1X-2, 0–2	1.51	161,918	692,267	80,252	1,713		32	tr				2,172
1X-4, 13–15	3.67	154,836	740,766	132,767	578		77					1,718
2X-3, 0–5	12.53	151,045	687,839	129,760	393		53	tr				2,442
3X-1, 0–5	19.03	188,098	757,871	39,861	5,701		10					3,908
3X-3, 0–5	22.03	176,566	783,687	33,947	1,684		16					2,095
4X-1, 95–100	29.48	179,080	762,634	50,447	3,533		34					1,497
6X-1, 145–150	40.48	153,340	667,552	38,213	2,601	tr.	31		0.8	tr.	1.8	1,063
7X-6, 0–5	56.03	127,472	698,926	58,799	9,700		43		1.9	4.5		990
8X-3, 145–150	62.48	103,641	719,730	60,327	5,420	1.0	41		6.8	5.1	3.4	884
9X-1, 0–5	67.53	162,469	645,999	61,564	5,420		281		39.4	32.6	31.4	132
9X-1, 64–69	68.17	114,746	710,498	10,015	5,420	0.9	339		17.0	15.8	15.4	22
11X-2, 10–15	79.63	143,192	704,554	35,800	334		264		35.8	38.3		103
12X-1, 60–65	88.13	167,365	781,741	25,299	6,451	tr.	167		29.4	20.4	2.6	106
13X-3, 96–101	100.99	176,890	1,028,848	20,081	4,741	tr.	121		23.1	28.5	tr.	107
13X-8, 0–5	103.45	162,343	1,055,523	61,304	4,849	tr.	186		29.4	31.5	3.9	215
14X-1, 6–11	106.59	173,101	718,681	32,385	1,147	tr.	249		58.8	47.1	20.5	80
14X-1, 20–25	106.73	147,248	781,741	12,530	2,941	tr.	327		116.2	45.1	31.3	22
15X-1, 98–100	116.99	146,993	686,294	47,617	11,138	tr.	354		102.8	50.2	5.0	87
16X-1, 41–43	125.92	191,269	925,261	19,513	4,060	tr.	525		267.5	109.5	52.8	18
17X-2, 0–3	135.61	207,599	808,947	61,211	3,056	tr.	302		33.9	10.2	2.6	169
18X-2, 0–5	146.03			11,856	3,056		188		50.4			50
20X-CC, 0–5	167.07	147,042	734,007	18,868	2,680		51		18.1	19.7	8.3	148
20X-2, 145–150	166.48	116,652	725,586	28,625	846		106		33.1	35.2	8.5	132
21X-1, 7–12	173.10	201,518	788412	95309	906		176		25.6	22.9	18.9	327
146-892D												
1X-1, 5–7	0.06	145,672	638,348	517	543		5		0.4			94
2X-1, 0–5	8.53	184,162	711,913	5,893	407		1		0.1			4,092
2X-2, 0–5	10.03	121,472	697,491	70,147	932		22					3,248
2X-2, 145–150	11.48	144,870	673,071	10,062	571		16		5.7	2.2	1.9	309
3X-1, 0–5	18.03	187,573	758,607	36,104	1,934		15		0.1			2,407
3X-2, 0–5	19.53	123,895	596,837	18,222	2,353		8		0.1			2,159
4X-2, 0–4	29.02	197,011	774,283	14,399	3,716		31		0.6			449
4X-3, 30–35	30.83	117,260	565,663	9,509	8,475		6		tr.			1,704
4X-3, 95–100	31.48	194,465	781,034	8,306	4,097		14		0.4	2.5		493
5X-2, 0–5	38.53	203,576	787,825	46,883	4,492		23		0.6			1,998
5X-3, 0–5	40.03	120,194	544,113	36,492	3,598		39		0.8			781
6X-4, 135–140	52.38	160,326	666,856	24,069	4,070	tr.	29		1.2			811
7X-4, 145–150	59.98	161,842	687,668	31,143	4,335		29		3.3	1.8		874
8X-3, 10–15	64.83	163,236	790,548	10,078	1,975	tr.	17		5.8	9.0	1.2	302
9X-4, 15–20	73.98	125,804	634,234	38,891	4,546		237		31.3	41.0	5.1	114
10X-4, 15–20	104.68	2,575	4,779	54,819	620		385		629.9	158.0	185.7	36
10X-6, 0–5	107.53	60,632	260,612	43,753	125		613		576.0	191.3	400.0	22
11X-1, 125–130	110.78	54,405	249,574	54,511	3,233		621		101.0	10.9	3.0	71
12X-4, 0–5	123.53	153,879	696,886	55,436	2,893		408		76.6	36.7	2.7	97
14X-2, 0–5	139.53	206,460	851,797	42,269	3,531		109		15.2	11.9		300
15X-3, 0–5	150.53	135,574	638,314	65,074	963	tr.	269		48.3	8.4		194
16X-3, 0–5	160.03	142,266	614,633	106,913	5155	tr.	247		30.8	19.2	3.1	345
146-892E												
1X-1, 0–5	0.03	42,504	249,592	730,754	3397	tr.	593		0.3	0.9		1,230
1X-1, 128–132	1.30	99,929	703,422	43,950	7116	tr.	31		0.6			1,384
1X-2, 125–130	2.78	80,713	381,245	542,390	4257	tr.	448		0.3	2.9		1,202
3H-5, 125–130	40.28	136,336	261,470	57,984	866	tr.	50		0.3	3.3		1,074
Headspace gases from hydrate dissociation in syringes												
146-892A												
1X-4, 13–15	3.67	178,369	872,556	66,408	504		30	11,733	1.4	21.2	1,182	
1X-4, 13–15	3.67	152,440	598,181	10,210	711		8	12,280	1.5	28.4	246	
1X-4, 13–15	3.67	209,043	890,491	36,026	274		12					3,116
1X-4, 13–15	3.67	165,080	747,892	46,085	731		22	12,408	1.5	31.0		840

Table 10. Vacutainer analyses for Hole 892A.

Core, section, interval (cm)	Depth (mbsf)	CH ₄	C ₂	C ₃	Area (Vs)	$\delta^{13}\text{CH}_4$ (‰)	Area (Vs) repl.	$\delta^{13}\text{CH}_4$ (‰) repl.
1X-2, 27–28	1.78	802,197	807.9		20.0	-66.1	18.3	-66.3
1X-3, 55–56	3.55	805,749	818.5		14.7	-67.5		
2X-4, 114–115	15.15	724,806	595.5		19.2	-66.3	8.9	-66.5
3X-2, 120–121	21.71	919,909	359.0	1.0	8.3	-66.3		
4X-2, 11–12	30.12	455,003	677.6	0.6	12.3	-67.9		
6X-2, 74–74	41.24	360,704	446.0	2.7			8.6	-68.3
6X-3, 148–148	43.48	851,695	993.7	6.1	9.4	-66.2	21.3	-66.0
7X-7, 22–22	57.72	854,304	2,070.0	11.1	15.7	-66.1		
8X-4, 135–135	63.85	848,342	1,155.0	32.6	14.5	-66.4	10.1	-66.1
11X-3, 26–27	81.26	931,873	6,322.0	273.0	8.0	-62.4	10.1	-63.5
13X-4, 66–67	102.17	949,757	5,310.9	205.3	12.7	-60.1	13.2	-60.1
15X-1, 84–84	116.84	648,209	7,137.0	3,473.0	9.9	-60.5	10.6	-60.5
17X-2, 63–63	137.13	811,411	6,201.0	332.2	11.6	-62.3	20.0	-61.2
18X-2, 6–7	146.07	139,571	352.9	29.4	5.6	-61.8		
20X-1, 147–148	164.98	390,854	1,007.0	102.0	8.8	-62.1	8.1	-62.5
G.HYDRATE-V.4	800,000				0.2	-64.8	0.5	-64.1
103/VAC900000PPM3/4	Standard	900,000	112,500.0	67,500.0	9.7	-36.5		
103/VAC900000PPM3/1	Standard	900,000	112,500.0	67,500.0	8.4	-36.5		
103/VAC900000PPM3/2	Standard	900,000	112,500.0	67,500.0	7.8	-36.3		
103/VAC900000PPM3/3	Standard	900,000	112,500.0	67,500.0	6.2	-36.2		
103/VAC300000PPM7/16	Standard	300,000	37,500.0	22,500.0	1.3	-37.4		
103/VAC900000PPM2/5	Standard	900,000	112,500.0	67,500.0	7.7	-36.6		
103/VAC900000PPM2/6	Standard	900,000	112,500.0	67,500.0	7.1	-36.2		
103/VAC300000PPM7/11	Standard	300,000	37,500.0	22,500.0	8.3	-36.7		
103/VAC300000PPM7/12	Standard	300,000	37,500.0	22,500.0	7.1	-39.4		
103/VAC300000PPM7/14	Standard	300,000	37,500.0	22,500.0	3.5	-36.6		
103/VAC300000PPM7/15	Standard	300,000	37,500.0	22,500.0	3.6	-36.6		

Note: repl. = replicate analysis.

Table 11. Total gas analyses for Hole 892A.

Core, section, interval (cm)	Depth (mbsf)	Type	Weight (g) frozen sediment	Area (Vs)	$\delta^{13}\text{CH}_4$ (‰)	CH ₄ (ppb wt) ngCH ₄ /g frozen sediment
20X-3, 0–10	166.5	VFG	3.45	7,1789	-63.5	2,399
20X-3, 0–10	166.5	VFG	3.45	6,5247	-63.7	2,181
20X-3, 0–10	166.5	VFG	4.2	7,4953	-63.8	2,252
20X-3, 0–10	166.5	VFG	4.2	6,8528	-63.9	2,059
18X-1, 140–150	145.9	VFG	2.57	5,4744	-64.0	2,763
18X-1, 140–150	145.9	VFG	2.57	2,5609	-63.5	1,293
15X-1, 88–100	116.9	VFG	1.55	1,4468	-60.8	1,173
13X-6, 69–82	101.6	VFG	2.13	3,4793	-64.2	2,089
11X-2, 0–10	79.5	VFG	1.83	5,0577	-63.2	3,349
9X-1, 69–74	68.2	VFG	5.24	6,0181	-63.8	1,356
8X-3, 0–10	61	VFG	0.94	0,9946	-63.2	1,328
8X-3, 0–10	61	VFG	0.75	0,8715	-63.5	1,335
6X-2, 0–10	40.5	VFG	0.94	2,6292	-65.9	3,574
3X-3, 0–10	21.8	VFG	1.1	0,6415	-60.4	688
2X-3, 0–11	12.5	VFG	2.44	1,1539	-61.9	572
2X-3, 0–11	12.5	VFG	2.23	1,3915	-61.4	901